

GENERALIZED RAY THEORY FOR SEISMIC WAVES IN STRUCTURES WITH PLANAR NONPARALLEL INTERFACES

BY PAUL G. RICHARDS, DEAN C. WITTE,* AND GÖRAN EKSTRÖM†

ABSTRACT

A discovery by Diebold (1987) can be used to show that there are analytical methods, developed and widely used for layers with plane parallel interfaces, that can often be extended to the case of plane interfaces that are not parallel. Layer interfaces can have arbitrary dip and strike, permitting the study of waves in truly three-dimensional structures.

We re-derive Diebold's result from first principles, showing that the travel time along a ray path is given by a summation of horizontal slowness times horizontal range and vertical slownesses times vertical "layer thicknesses," in a form essentially identical to the standard relationship between these quantities in a medium that is laterally homogeneous.

We then show that, because of an underlying lateral invariance in the ray relationships within a stack of wedge-shaped layers, it is simple to develop a generalized ray theory for wave propagation in such a medium. Finally, we show how such a theory can readily be used to synthesize body-wave pulse shapes at teleseismic distances, in a spherically symmetric Earth modified by dipping structures in the vicinity of source and/or receiver.

INTRODUCTION

We outline a generalized ray theory for structures consisting of a stack of homogeneous layers that meet on planar interfaces of arbitrary dip and strike. A rapid procedure is then suggested for finding the rays, travel times, and geometrical spreading in such a model without the need to carry out raytracing. The effects of intrinsic attenuation in each layer (or wedge) can easily be accommodated, and the method appears suitable for further generalizations that extend Cagniard-de Hoop theory and other generalized ray theories such as disk ray theory (Wiggins, 1976; Chapman, 1976) to waves in layering with arbitrary dip and strike.

The basis for our approach is a formula derived by Diebold (1987), giving the travel time along a ray path between two points in a stack of homogeneous layers with interfaces of arbitrary dip and strike. He proved that this time is

$$T = \mathbf{p}_A \cdot \mathbf{X}_A + \mathbf{p}_B \cdot \mathbf{X}_B + \sum_j (\xi_{aj} + \xi_{bj}) z_j, \quad (1)$$

where (see Fig. 1) \mathbf{p}_A is the horizontal slowness of the ray departing from a source at \mathbf{A} ; \mathbf{X}_A is the horizontal vector from \mathbf{A} to a vertical reference line on

* Present address: Chevron Oil Field Research Company, P.O. Box 446, La Habra, California 90633-0446.

† Present address: Department of Geological Sciences, Harvard University, Cambridge, Massachusetts 02138.

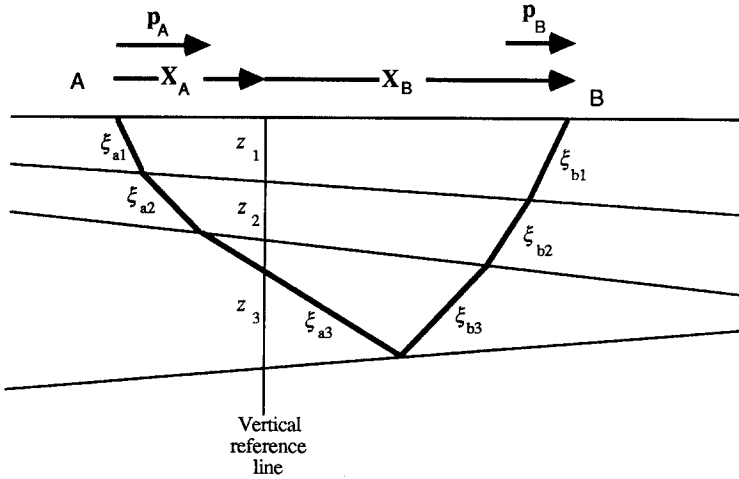


FIG. 1. "Layer thicknesses" are defined by intersection of interfaces with a vertical reference line. This is a 2-D schematic of a 3-D ray path from A to B that is composed of line segments that in general are not co-planar. Dipping interfaces are planar but are not presumed to share a common strike. Notation is shown for vertical slownesses in each layer.

which layer thicknesses z_j are defined; ξ_{aj} is the vertical slowness in the j th layer for the downward ray segments and ξ_{bj} are the upward vertical slownesses (the summation is just for those layers traversed by the ray); and \mathbf{p}_B and \mathbf{X}_B are respectively the horizontal slowness and horizontal position vector from the vertical reference line, to a receiver at B. We shall be using boldface symbols for 2-D and 3-D vectors, and note that \mathbf{p} and \mathbf{X} are horizontal 2-D vectors, so that the 3-D slowness \mathbf{s} is given by $\mathbf{s} = (\mathbf{p}, \xi)$.

Diebold's formula has long been known for the case of parallel layering, when it is trivial to prove from the integral of slowness,

$$T = \int_{\text{ray}} \mathbf{s} \cdot d\mathbf{l},$$

in which $d\mathbf{l}$ is an element of length along the ray. In cartesian coordinates with x horizontal in the plane of propagation and z in the depth direction, components of slowness are $\mathbf{s} = (p, 0, \xi)$ with p a scalar constant along the ray (i.e., Snell's law); and $d\mathbf{l} = (dx, 0, dz)$. It follows for such one-dimensional structures that the travel time to the receiver at range X is

$$T = \int_{\text{ray}} (p, 0, \xi) \cdot (dx, 0, dz) = pX + 2 \sum_j \xi_j z_j = pX + \tau(p). \quad (2)$$

The τ function here is the integral of vertical slowness ξ over the depth range spanned by the ray: τ is often called the intercept time, because, from equation (2) $\tau = T(p) - pX(p)$, which is the time intercepted on the time axis by the tangent to a travel-time curve (T versus X).

A formula similar to (1) has been known for several years for 2-D problems, i.e., for structures composed of homogeneous layers in contact on planes with arbitrary dip but all having a common strike direction, and with ray paths

confined to the vertical plane perpendicular to that strike (Adachi, 1954; Johnson, 1976; Hong and Helmberger, 1977; Diebold and Stoffa, 1981). It is remarkable, as Diebold (1987) showed, that equation (1) still applies even for 3-D problems where the planar interfaces have arbitrary dip *and* strike. The total ray path is then composed of a series of straight line segments, with Snell's law applying locally on each interface between layers. The net result in 3-D is a ray that is no longer confined to a single plane, let alone a vertical plane. The propagation path thus becomes much more difficult to draw, though conceptually there is little difficulty in tracing the ray from layer to layer, starting with a given "take off" direction (specified by \mathbf{p}_A ; or, equivalently, by azimuth and magnitude of the horizontal phase velocity at the source). In equation (1), the vertical slownesses differ, in general, for downward and upward ray segments in the same layer. The vertical reference line is fixed but can initially be chosen anywhere (e.g., through the source or at the receiver). Layer thicknesses z_j (see Fig. 1) will differ, as will \mathbf{X}_A and \mathbf{X}_B , for different choices of this reference line. But choices here do not influence the slowness components \mathbf{p}_A , \mathbf{p}_B , ξ_j .

Diebold (1987) gave a trigonometrical proof of equation (1). The result is surprisingly simple, yet apparently had not been previously recognized for 3-D applications. In the following section, his result is demonstrated from first principles with the intent of showing that a proof is hardly needed when the overall ray path is decomposed in a particular way; the result itself can simply be written down as self-evidently true. A procedure is then outlined, for determining sequentially the vertical slownesses ξ_j along the ray path. This does not require raytracing.

It is well known that equation (2), used as a Cagniard path, leads to a generalized ray representation for parallel interfaces (including the effect of headwaves if present). We will show that an outcome of Diebold's result is a generalized ray theory for media with planar-dipping interfaces. In 3-D problems this is likely, as a minimum, to give an effective procedure for computing ray paths, travel times, and geometrical spreading. There is no need to iterate, to fit a ray between a particular source and receiver. If desired, attenuation (intrinsic dissipation) can readily be incorporated in the calculation of amplitudes. Other generalizations of the theory for parallel interfaces to 3-D structures are likely to include Cagniard-de Hoop analysis of refractions (headwaves) along dipping interfaces and related extensions to WKB theory. We compare the predictions of our method (i.e., the synthetics) with those of geometrical ray theory for a simple problem of reflection from a single-dipping interface. We also show how to adapt the method to quantify the effect on body waves in a spherically symmetric Earth due to dipping structure near source and/or receiver.

THE BASIC RELATION BETWEEN TRAVEL TIME AND SLOWNESSES

In this section, we show that the 3-D travel-time result, equation (1), can readily be written down even in complicated situations where layers may pinch out, where there is different layering beneath source and receiver, where *P-S* conversions may occur, and when refractions and/or multiple legs are permitted in a particular layer. We then show explicitly how to account for changes in horizontal slowness along a ray path, by taking a sequence of square roots that (for planar interfaces) is laterally invariant.

Proof of the Basic Travel-Time Formula

We begin with a simple problem, of one reflection from an interface as shown in Figure 2. The source (at A) and the receiver (at B) are on the same horizontal free surface, and the ray travels wholly within a homogeneous isotropic layer with seismic body-wave speed v . In this case, both 3-D slowness vectors \mathbf{s}_A , \mathbf{s}_B have magnitude $1/v$. For general dip and strike, the plane of the two ray segments need not be vertical. To obtain the travel time along the ray, consider a plane wavefront moving perpendicular to the ray. We shall accumulate the total travel time, by following the intersection of this wavefront with either horizontal or vertical lines. Thus, we identify points M_1 , N_1 , M_2 between A and B on the ray path (see Fig. 3), which are positions such that the wavefront is in turn at X_{ref} , Z , and X_{ref} (again). The time to propagate from A to M_1 is $\mathbf{p}_A \cdot \mathbf{X}_A$ because this is the time for the same wavefront to propagate in the horizontal plane along \mathbf{X}_A (i.e., to X_{ref}) with horizontal slowness \mathbf{p}_A . The time to propagate from M_1 to N_1 is $\xi_A z$, because this is the time for the wavefront to propagate down the vertical reference line from X_{ref} to Z with vertical slowness ξ_A . The time from N_1 to M_2 via R equals the time from N_2 to M_2 with speed v (from the equality of N_1R and N_2R claimed in the Fig. 3 caption), which is $\xi_B z$ because the wavefront is moving from Z up to X_{ref} with vertical slowness ξ_B . Finally, the time from M_2 to B is $\mathbf{p}_B \cdot \mathbf{X}_B$, as the wavefront propagates horizontally from X_{ref} to B . From breaking the travel time down into four successive steps, it follows that

$$T = \mathbf{p}_A \cdot \mathbf{X}_A + \mathbf{p}_B \cdot \mathbf{X}_B + (\xi_A + \xi_B) z,$$

which is a simple example of equation (1).

Next, consider two additional levels of complication as shown in Figure 4. Here, the source at A is not necessarily on the same horizontal level as the receiver at B . The downgoing ray is transmitted across another dipping inter-

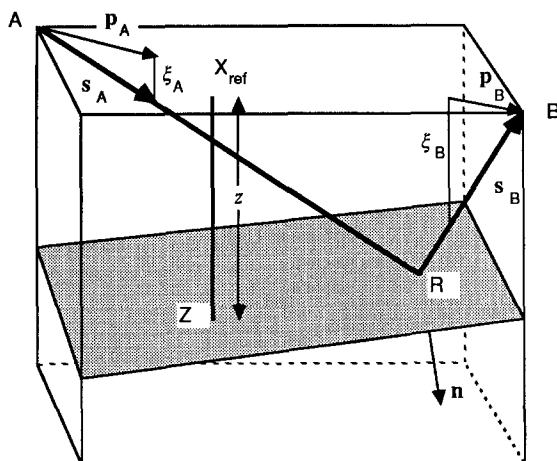


FIG. 2. A ray is shown, reflected at the point R on a planar interface with normal \mathbf{n} . Incident and reflected slownesses are \mathbf{s}_A and \mathbf{s}_B . These 3-D vectors have horizontal components \mathbf{p}_A , \mathbf{p}_B (2-D vectors in the horizontal plane). Vertical slownesses are ξ_A and ξ_B (scalars). A vertical reference line, from a point X_{ref} in the horizontal surface, meets the dipping interface at the point Z .

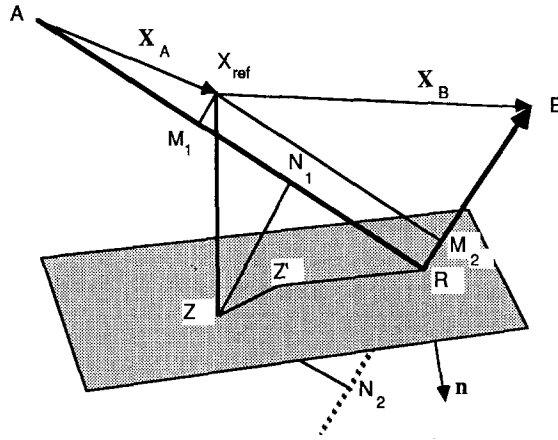


FIG. 3. Another view of the reflected ray shown in Figure 2. Lines $M_1 X_{ref}$, $N_1 Z$ are perpendicular to the incident ray (AR). Line $M_2 X_{ref}$ is perpendicular to the reflected ray (RB). Lines ZN_1 , ZN_2 are perpendiculars to the incident ray and to a continuation of the reflected ray. Lengths $N_1 R$, $N_2 R$ are equal. This can best be seen by dropping a perpendicular from Z to the plane containing s_A , s_B , and n (the normal to the dipping reflector). The foot of the perpendicular is Z' , and it too must lie in the dipping plane. Points Z' , N_1 , R , N_2 , lie in the same plane, and equality of $N_1 R$ and $N_2 R$ follows from equality of angles of incidence and reflection ($s_A \cdot n = -s_B \cdot n$).

face, beneath a layer that pinches out so that it is not traversed by the eventual upgoing ray, which is reflected from a deeper dipping surface.

Ray segments AR_1 , $R_1 R_2$ lie in the same plane as n_1 (the normal to the dipping refractor). Z_1' is defined to lie in this plane, at the foot of the perpendicular from Z_1 . It follows that Z_1' also lies in the refracting interface. To get the overall travel time from A to B , consider again a plane wavefront moving along (and perpendicular to) the ray. The time from A to L_1 is $p_A \cdot X_A$. The time from L_1 to M_1 is more interesting. It equals the time from L_1 to L_2 using the speed of the first ray segment, because the time from R_1 to L_2 at this speed equals the time from R_1 to M_1 at the speed of the refracted ray. This last equality is a direct consequence of Snell's law: the time from R_1 to L_2 for the incident ray equals the time for the wavefront to propagate obliquely from R_1 to Z_1' . All refracted or reflected wavefronts, including cases of conversion between P and S waves, are coupled on the interface and travel along it at the same speed. So, the time taken for oblique propagation at this speed, as any of these coupled wavefronts moves from R_1 to Z_1' , equals the time to travel directly along one of the rays, to the point (such as M_1) where the associated wavefront will then also lie on Z_1' . Such a wavefront will then also lie on Z_1 . The remainder of the path, from M_1 to R_2 and reflection to B , is similar to the discussion of Figure 3. We can get the overall travel time, from L_1 to M_2 , by tracking on the vertical reference line the position of the wavefront moving perpendicular to the ray. Travel time along these segments is given schematically in Figure 5, and we find the exact result

$$T = p_A \cdot X_A + p_B \cdot X_B + \sum_{\text{ray}} \xi_j z_j. \tag{3}$$

Equation (3) is almost the same as Diebold's (1987) result (equation 1 above) but brings out the obvious generality that downgoing and upgoing ray legs need

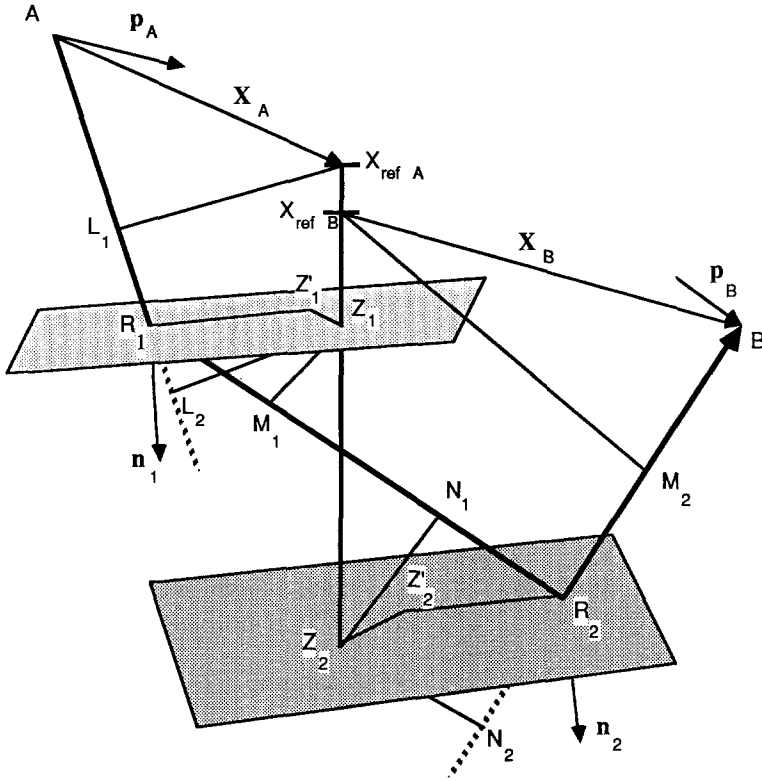


FIG. 4. The ray shown here from A to B is refracted at R_1 and reflected at R_2 . A vertical reference line meets the two dipping interfaces at Z_1 and Z_2 . $X_{ref A}$, $X_{ref B}$ lie on this vertical line, at the horizontal levels of A and B , respectively. For a plane wavefront propagating perpendicular to the ray, locations at L_1 , M_1 , N_1 , and M_2 would put the wavefront also, in turn, at $X_{ref A}$, Z_1 , Z_2 , and $X_{ref B}$. $Z_1 L_2$ and $Z_2 N_2$ are perpendiculars to parts of the ray that are extrapolated out of the layer in which the real ray path is defined.

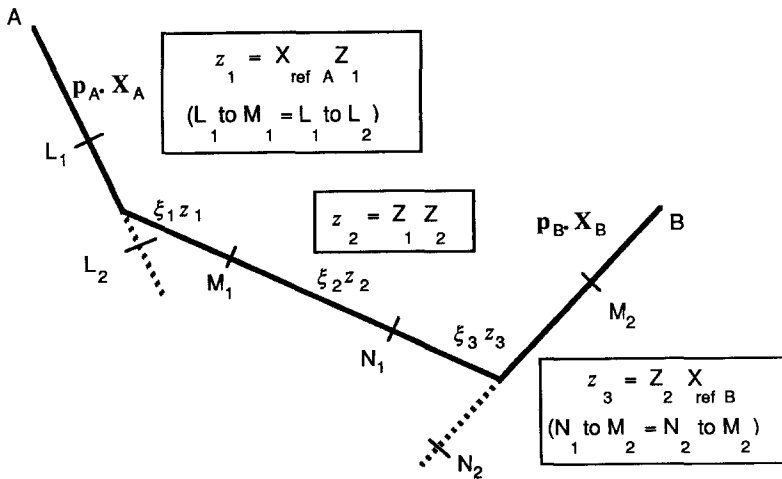


FIG. 5. Schematic of the ray path for Figure 4, showing propagation times for different segments. The z_i are effective layer thicknesses. Note: the three ray legs of the overall path would not in general lie in the same plane.

not cross the same interfaces. Pinchouts may occur. It is clear too that the method of proof can handle conversion between P and S , at any reflection or transmission. Thus, for each of the five rays shown in Figure 6, associated wavefronts have the same phase velocity along the interface in the direction RZ' (i.e., along the interface and in the plane containing \mathbf{n} and the five rays). This is the most basic expression of Snell's law. It follows that the time taken to travel from R to each of the points P_i ($i = 1, 2, 3, 4$) at speed v_i , where v_i is the body-wave speed appropriate for the ray passing through P_i , is equal to the time taken to travel from R to P_0 at speed v_0 , where v_0 is the body-wave speed of the incident wave. This result is generalized to 3-D, by noting that instead of defining each P_i via perpendiculars from a point Z' as shown, we could choose any point Z in the interface (in general, lying out of the plane of the rays), from which to drop all the perpendiculars. The time to travel from R to each P_i would still be equal.

In forming the sum, $\sum \xi_j z_j$ in equation (3), it is necessary only to choose the vertical slowness appropriately, whether for P or S , in each straight line ray segment. In forming the sum, $\sum \xi_j z_j$, it may seem natural to take positive signs always for the vertical slowness and for the layer thickness. For example, ξ_j and z_j would both appear to be positive for downgoing ray segments. Exceptions such as one shown in Figure 7 may occur. To the extent that a sign change appears appropriate for upgoing segments, each of ξ_j and z_j appears to require a sign change and so these changes might be ignored since the product is not affected. (Note: the effects of the factor $(\xi_{aj} + \xi_{bj})$ in equation (1) and the factor 2 in equation (2), are included in equation (3) because the latter equation is taken along the ray path and the former two equations are taken over depth.) However, in complicated situations where it is more difficult to keep track of signs, a more systematic procedure is required, as we next discuss.

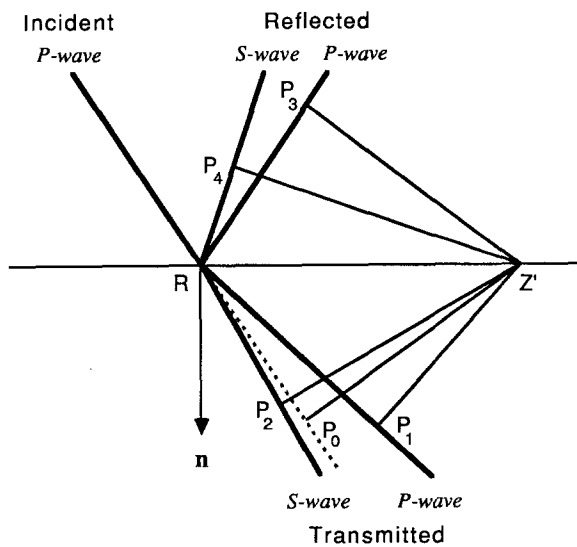


FIG. 6. The scattered waves are shown for a P -wave incident at point R on a planar interface with normal \mathbf{n} . Z' is any point lying both in the plane of the rays and the interface. The dashed line is a continuation of the incident ray, and points P_i lie on perpendiculars drawn from Z' .

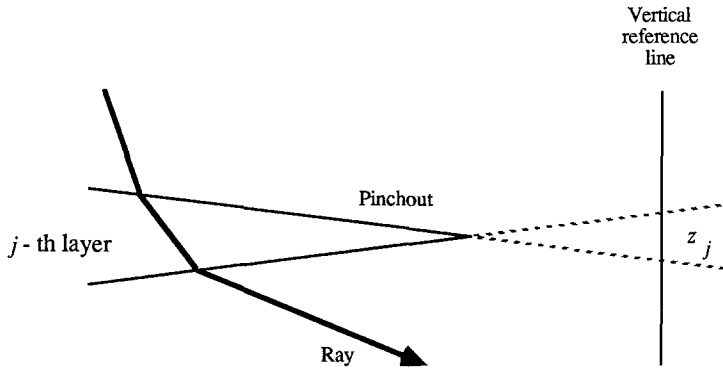


FIG. 7. Schematic in 2-D, for a 3-D situation in which pinchout occurs. The vertical reference line meets extrapolations of the two interfaces, defining a "layer thickness" that would enter equation (3) with a negative value if the ray passed down through the j th layer (i.e., $\xi_j > 0$, $z_j < 0$, in this case).

Sequential Evaluation of Vertical Slownesses

For horizontal plane layering, vertical slownesses are simply $\sqrt{(v^{-2} - p^2)}$ in a layer with body-wave speed v (whether for P or S): the scalar horizontal slowness p , also called the ray parameter, is (by Snell's Law) unchanged throughout the medium. We shall refer to this as the 1-D problem. It has been studied for decades. (See Spencer, 1960, and Helmberger, 1968, for discussion of generalized rays; Chapman and Orcutt, 1985, and Aki and Richards, 1980, Chapters 5, 6, 7, 9.)

For the 3-D problem, horizontal slowness should be thought of as a 2-D vector, and it is changed in general from one ray segment to the next, since interfaces need not be horizontal. For applications of equation (3), it is useful to have each vertical slowness ξ_j defined in terms of the initial horizontal slowness \mathbf{p}_A , at the source. (In some cases of data analysis, for example when \mathbf{p}_B is a measured quantity, the horizontal slowness at the receiver is the more natural independent variable.)

For the 3-D problem, let the sequence of layers traversed by the ray have, in turn, body-wave velocities $v\hat{A} = v_0, v_1, v_2, v_3, \dots, v_j, \dots, v_J = v\hat{B}$ (see Fig. 8). At some interfaces there is reflection; at others, transmission. Some velocities in the list may be equal (e.g., adjacent velocities are equal for a P -wave reflection). The list can be a mix of P - and S -wave velocities, signifying conversion on reflection or transmission. A generalized ray is specified by this list, together with designation of the interaction occurring at each interface (reflection or transmission, conversion or no conversion).

Let the normals for interfaces "met" by the ray path be $\mathbf{n}_1, \mathbf{n}_2, \mathbf{n}_3, \dots, \mathbf{n}_j, \dots, \mathbf{n}_J$. The remaining details of Earth structure concern layer thicknesses, specified by the sequence $z_1, z_2, z_3, \dots, z_j, \dots, z_J$ of "layer thicknesses" measured on the vertical reference line between interfaces (extrapolated as necessary, for pinchouts; see Fig. 7).

The travel-time formulas, equations (1) or (3), do not require explicit knowledge of the length of ray segments in each layer. It is relatively simple to work out the sequence of slowness vectors $\mathbf{s}_0, \mathbf{s}_1, \mathbf{s}_2, \mathbf{s}_3, \dots, \mathbf{s}_j, \dots, \mathbf{s}_J$ on each of the $J + 1$ ray segments, since this does not depend on layer thicknesses or lateral

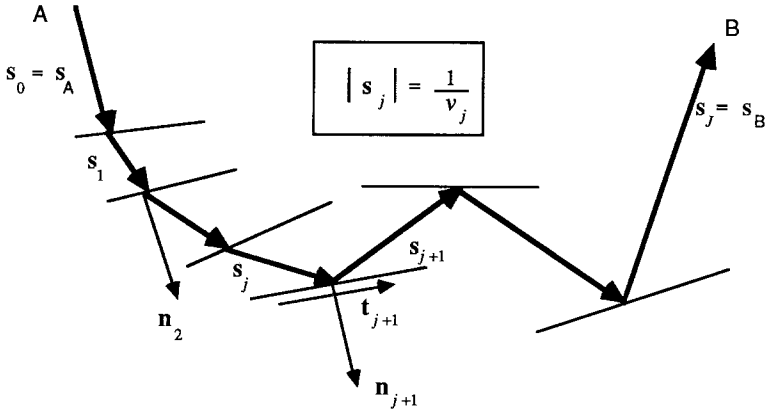


FIG. 8. 2-D schematic of a 3-D ray path, showing the labeling of layer velocities, slowness vectors, and interface normals. Interface $j + 1$ lies between layers j and $j + 1$. We here presume that source and receiver lie on horizontal surfaces (the zero-th and $J + 1$ th “interfaces,” with normals $\mathbf{n}_0, \mathbf{n}_{J+1}$ that are vertical). Let Z_j be the depth of the point on the vertical reference line cut by the j th interface. Then, the “thickness” z_j of the j th layer is $Z_{j+1} - Z_j$. Vertical slowness ξ_j is the z component of \mathbf{s}_j . In forming $\xi_j z_j$ with these definitions, note that vertical slownesses and “layer thicknesses” can be negative.

position. It does, of course, depend on the sequence of interface orientations. When specifying vector components in detail, for slowness \mathbf{s} and interface normals \mathbf{n} , a useful right-handed coordinate system is (North, East, Down) for (x, y, z) . Thus, for conventional definitions of dip δ , measured down from horizontal, and strike ϕ_s , measured clockwise round from North, the components of \mathbf{n} are $(\sin \delta \sin \phi_s, -\sin \delta \cos \phi_s, \cos \delta)$. (See Aki and Richards (1980) Fig. 4.13 for a convention on ranges of δ and ϕ_s ; in what follows, \mathbf{n} always has a nonnegative z component.)

We are now in a position to give the sequence of vertical slownesses $\xi_0, \xi_1, \xi_2, \xi_3, \dots, \xi_j, \dots, \xi_J$ given the initial horizontal slowness vector \mathbf{p}_A with (North, East) components (p_{Ax}, p_{Ay}) .

Thus, since

$$\mathbf{s}_0 = (p_{Ax}, p_{By}, \xi_0) \quad \text{and} \quad |\mathbf{s}_0| = \frac{1}{v_0}, \tag{4}$$

it follows that

$$\xi_0 = \sqrt{\frac{1}{v_0^2} - p_{Ax}^2 - p_{Ay}^2}, \tag{5}$$

so \mathbf{s}_0 and ξ_0 are known as functions of $(p_{Ax}, p_{Ay}) = \mathbf{p}_A$.

In general (see Figs. 8 and 9), \mathbf{s}_j and \mathbf{s}_{j+1} are related by the rule

$$\mathbf{s}_j - (\mathbf{s}_j \cdot \mathbf{n}_{j+1})\mathbf{n}_{j+1} = \mathbf{s}_{j+1} - (\mathbf{s}_{j+1} \cdot \mathbf{n}_{j+1})\mathbf{n}_{j+1} = \mathbf{t}_{j+1}. \tag{6}$$

This is an expression of Snell’s Law, equating the projection (along the interface) of incident and scattered wave slownesses. Equation (6) defines \mathbf{t}_{j+1} , the along-interface slowness vector (Fig. 8 or 9). The equation can be turned into a

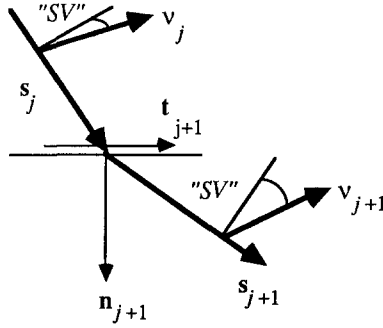


FIG. 9. The direction of vector \mathbf{S} motion is quantified by unit vectors $\mathbf{v}_j, \mathbf{v}_{j+1}$, transverse to the ray. Vectors $\mathbf{s}_j, \mathbf{s}_{j+1}, \mathbf{n}_{j+1}, \mathbf{t}_{j+1}$ all lie in a common plane, labeled Π (say); the projection of \mathbf{v}_j in this plane gives the fraction of incident S displacement that locally is "SV." Vector subtraction of this in-plane component, or alternatively the projection of \mathbf{v}_j on to the normal to Π , gives the incident local "SH" component.

explicit expression for \mathbf{s}_{j+1} in terms of \mathbf{s}_j , noting that

$$\mathbf{s}_{j+1} \cdot \mathbf{n}_{j+1} = \pm \sqrt{\frac{1}{v_{j+1}^2} - \mathbf{t}_{j+1} \cdot \mathbf{t}_{j+1}}, \tag{7}$$

where the positive root is taken if the ray departs from the interface on the same side as \mathbf{n} , and the negative root if departure is on the other side from \mathbf{n} . Combining the last two equations,

$$\mathbf{s}_{j+1} = \mathbf{s}_j - (\mathbf{s}_j \cdot \mathbf{n}_{j+1})\mathbf{n}_{j+1} \pm \sqrt{\frac{1}{v_{j+1}^2} - \frac{1}{v_j^2} + (\mathbf{s}_j \cdot \mathbf{n}_{j+1})^2} \mathbf{n}_{j+1} \tag{8}$$

and

$$\xi_{j+1} = z \text{ component of } \mathbf{s}_{j+1} = \mathbf{s}_{j+1} \cdot (0, 0, 1). \tag{9}$$

Equations (4) through (9) give a method for computing all relevant vertical slownesses along the generalized ray path, as a function of the initial horizontal slowness components, $\mathbf{p}_A = (p_{Ax}, p_{Ay})$. The magnitude of each of the \mathbf{t}_{j+1} is all that is needed locally to evaluate specific reflection/transmissions coefficients (see Aki and Richards, 1980, Chapter 5, for detailed formulas for these coefficients). If \mathbf{p}_B is needed, it can be found from the horizontal components of \mathbf{s}_j .

For S waves, the question of polarization also arises (see Fig. 9). Between interfaces j and $j + 1$ for an S wave, let particle motion be in the direction \mathbf{v}_j (a unit vector, perpendicular to \mathbf{s}_j because the motion is transverse to the ray). The projection of \mathbf{v}_j on to the plane containing $(\mathbf{s}_j, \mathbf{s}_{j+1}, \mathbf{n}_{j+1}, \mathbf{t}_{j+1})$ then gives the fraction of S displacement to be regarded locally as incident SV. Incident SH is given by a vector subtraction. On emergence from the interface, separately using SV and SH coefficients of reflection or transmission for the local SV and SH components, vector \mathbf{S} displacement is reconstituted from local SV and SH to determine the new direction \mathbf{v}_{j+1} of transverse particle motion propagated with slowness \mathbf{s}_{j+1} to the next interface.

Note that computations for the sequence of slowness vectors (and for the directions of particle motion) depend only on wave speeds in each layer and on the orientations of interfaces. Specifically, these computations do not depend on layer thicknesses. Because of this invariance, one can say that the forward computation of travel time, for a given source and a given take-off direction, can be done without raytracing. It appears that in general one does not know what receiver positions will be reached by this ray. However, in the next section, it is shown how to find the take-off direction for a ray that reaches a particular receiver.

RAY CALCULATIONS WITHOUT RAYTRACING

1-D

There are many conceivable uses of the exact travel-time formula, equation (3). An elementary use concerns fitting a ray between a fixed source and receiver and finding the geometrical spreading, without actually doing any raytracing. To illustrate this use, the method will first be reviewed for the problem of rays in 1-D structures.

Thus, in the frequency domain, the wave field for a generalized ray in a structure that varies solely with depth can be written

$$W(X_0, \omega) = \int_{\Gamma} f(p, \omega) \exp[i\omega\{T(p, \omega) - pX(p, \omega) + pX_0\}] dp, \quad (10)$$

where Γ is a path of integration in the p plane (see Aki and Richards, 1980, Chapter 9); $T(p, \omega) - pX(p, \omega)$ is the vertical integral of vertical slowness along the ray path,

$$T - pX = \tau = \int_{\text{ray}} \sqrt{\frac{1}{v^2} - p^2} dz, \quad (11)$$

in which $v(z)$ is the velocity (complex, if there is attenuation, and frequency dependent if there is dispersion); and $f(p, \omega)$ includes the radiation pattern as well as relevant reflection/transmission coefficients for the generalized ray of interest.

Both plane-stratified and spherically stratified media can be studied via (10). Richards (1973) obtained examples of equation (10) even for rays that have turning points, rather than reflection from a specific interface. Following the discussion by Aki and Richards (1980), their equation (9.41), but with the notation of equation (10), we here expect stationary points to occur at values p_0 of the ray parameter, which are solutions of the equation $X(p) = X_0$.

In order to obtain the ray-theory approximation for an array of receivers, consider the following six steps.

(1) One fixes ω and computes f and $\tau(p)$ for a set of equally spaced real p values, in a range of the real ray-parameter axis that is close to where one expects complex saddle points to lie, for the range of distances (i.e., X_0 values) at which one wishes to know W . Let the increment in p be Δp .

(2) At fixed X_0 , one searches through the sampled values of $\text{Real}[T - pX + pX_0]$ to see at which of the discrete points in p it has its least value (or greatest value, for certain kinds of ray). Label this discrete point as p_{js} . The complex

saddle must lie near this point of the real p axis. If there is no attenuation, the saddle will lie on the real p axis if there is a real ray between source and receiver.

(3) Find the values (complex, if there is attenuation) of the three constants T_0 , p_0 , and $DXDP$ that best fit the sampled phase factor according to

$$T - pX + pX_0 = T_0 - \frac{1}{2}(p - p_0)^2 \times DXDP \quad (12)$$

in the vicinity of p_{j_s} . In this way, one obtains in p_0 an estimate of the position of the complex saddle; in T_0 an estimate of the complex travel time; and in $DXDP$ (signifying dX/dp at the saddle) an estimate of the relevant constant, complex in general, needed to evaluate geometrical spreading. Note that, if one just uses p_{j_s} itself and the points just before and just after it, closed form expressions that in practice are often very accurate can easily be given for p_0 , T_0 , and $DXDP$. Aki and Richards (1980) define the function $J(p) = T - pX + pX_0$ (see their page 423). In terms of this sampled function, the closed form expressions for the desired constants are

$$\begin{aligned} DXDP &= -[J_{j_s+1} - 2J_{j_s} + J_{j_s} - 1]/(\Delta p)^2, \\ p_0 &= p_{j_s} + [J_{j_s+1} - J_{j_s-1}]/(2 \cdot \Delta p \cdot DXDP), \\ T_0 &= J_{j_s} + (p_{j_s} - p_0)^2 \times DXDP/2. \end{aligned} \quad (13)$$

(4) Interpolate from $f(p_{j_s}, \omega)$ and $f(p_{j_s+1}, \omega)$ to evaluate $f(p_0, \omega)$.

(5) Claim that the saddle point approximation to W is

$$W(X_0, \omega) = f(p_0, \omega) \sqrt{\frac{2\pi}{i\omega DXDP}} e^{i\omega T_0}. \quad (14)$$

Choose the next value of X_0 , and loop back to the second step to do various distances. Choose the next value of frequency ω , and loop back to the first step. This loop is necessary only if Q is frequency dependent and if there is allowance for body-wave dispersion. For some types of anelasticity, it may be possible to abbreviate this step and estimate more directly the global frequency dependence of the saddle-point approximation.

(6) Finally, one can go to the time domain:

$$W(X_0, t) = \frac{1}{2\pi} \int_{-\infty}^{\infty} W(X_0, \omega) e^{-i\omega t} d\omega. \quad (15)$$

Note that the whole effort is accomplished using real values of ray parameter, at the time-consuming stage of tabulating f and τ at discrete p values. Often, the dependence on frequency in equation (14) is sufficiently simple that equation (15) can be evaluated explicitly. Since the final time series is real, (15) can be addressed using only positive frequencies.

The method allows easily for investigation of different attenuation-dispersion pairs. This is handled just by insertion of some appropriate rule for evaluating a complex, frequency-dependent "velocity" $v = v(z, \omega)$ and making allowance in equations (10) through (13) for the fact that $\tau = \tau(p, \omega)$. The method is simple

and rapid to execute, and has been found quite accurate for 1-D problems (Richards, 1985, pages 197 to 199).

A series of papers by Borchardt (including Borchardt *et al.*, 1986; see also Richards, 1984) has drawn attention to the need for more careful handling of attenuation. Specifically he has advocated working with plane waves that may propagate in a direction that differs from the direction of most rapid attenuation. (The “direction of propagation” is the direction of most rapid phase increase.) He has shown that such waves have properties that much conventional analysis (i.e., that based on plane waves propagating in the direction of maximum attenuation) cannot reproduce. Fortunately, the method based on equations (10) through (14), which finds stationary values of the integrand at complex values of horizontal slowness, gets around Borchardt’s objections to conventional analysis, yet does so for attenuating media in a way that requires little change from computational experience with elastic media.

3-D

The essence of each of steps (1) through (6) carries over to 3-D problems in layered structures with dipping planar interfaces. The major differences concern the need to work with two components of horizontal slowness, $(p_{Ax}, p_{Ay}) = \mathbf{p}_A$. Outlining part of the theory in a particularly simple case, let us choose the vertical reference line to lie through the receiver so that $\mathbf{p}_B = 0$. Without ambiguity we can then drop the subscript *A* from \mathbf{p}_A , writing $\mathbf{p} = (p_x, p_y)$ for the horizontal slowness at the source. We now have two scalar independent variables, and it is instructive to use them to reproduce the known field of a point source in a homogeneous medium. Thus, consider

$$W(\mathbf{X}_0, \omega) = \frac{\exp\left(i\omega \frac{R}{\alpha}\right)}{R}, \quad \text{where } R = |\mathbf{X}_0|,$$

which describes a spherical wave at $\mathbf{X}_0 = (X_0, Y_0, Z_0)$, expanding from the origin.

Then it is known that *W* can be expressed as

$$W(\mathbf{X}_0, \omega) = \frac{i\omega}{2\pi} \int_{-\infty}^{\infty} \int_{-\infty}^{\infty} \frac{1}{\xi} \exp[i\omega(p_x X_0 + p_y Y_0 + \xi |z|)] dp_x dp_y, \quad (16)$$

where $\xi = \sqrt{1/v^2 - p_x^2 - p_y^2}$. For derivation of a related result, see Aki and Richards (1980, pages 197 to 199).

Defining *J* by

$$J(p_x, p_y) = \mathbf{p} \cdot \mathbf{X}_0 + \tau(p_x, p_y),$$

which equals $p_x X_0 + p_y Y_0 + \xi |z|$ here in (16), we can expect to find an expansion about the stationary point as

$$J(p_x, p_y)$$

$$= T_0 + A(p_x - p_{x0})^2 + 2B(p_x - p_{x0})(p_y - p_{y0}) + C(p_y - p_{y0})^2. \quad (17)$$

In the present case, because it is so simple, we know $T_0 = R/\alpha$, and we can even find analytic expressions for the Taylor series coefficients. They are

$$A = -\frac{|z|}{2\xi_0^3} \left(\frac{1}{v^2} - p_{y0}^2 \right), \quad B = -\frac{|z|}{2\xi_0^3} p_{x0} p_{y0}, \quad C = -\frac{|z|}{2\xi_0^3} \left(\frac{1}{v^2} - p_{x0}^2 \right).$$

But in the general case, using a table of values for $\tau(p_x, p_y)$, the six constants $T_0, A, B, C, p_{x0}, p_{y0}$ may be recovered numerically, using essentially the same method as given in equations (12) and (13) for a scalar horizontal slowness. The stationary phase approximation is

$$W(\mathbf{X}_0, \omega) = \frac{i\omega e^{i\omega T_0}}{2\pi\xi_0} \int_{-\infty}^{\infty} \int_{-\infty}^{\infty} \exp\left[i\omega \left\{ A(p_x - p_{x0})^2 + 2B(p_x - p_{x0})(p_y - p_{y0}) + C(p_y - p_{y0})^2 \right\} \right] dp_x dp_y, \quad (18)$$

and after some straightforward work it can be shown that this double integral is merely

$$\int_{-\infty}^{\infty} \int_{-\infty}^{\infty} \exp[\{\dots\}] dp_x dp_y = -\frac{i\pi}{\omega} \sqrt{\frac{1}{AC - B^2}}. \quad (19)$$

Substitution of equation (19) into (18) gives an analytic approximate solution for $W(\mathbf{X}_0, \omega)$ that is easily taken into the time domain. In the present case, where explicit formulas for A, B, C are known, we can go on to show that $\sqrt{[1/(AC - B^2)]} = 2\xi_0^2 \cdot v/|z|$, and, since $\xi_0 \cdot v/|z| = 1/R$, it turns out for the point source in a homogeneous medium that the stationary phase approximation returns the exact solution,

$$W(\mathbf{X}_0, \omega) = \frac{\exp\left(i\omega \frac{R}{\alpha}\right)}{R}.$$

Having given elementary results in this section for a 1-D medium, and for a point source regarded as an integral over two horizontal slownesses, equation (16), we next give some more general results for the 3-D problem.

A REPRESENTATION FOR GENERALIZED RAYS

For a generalized ray in a stack of layers with randomly dipping planar interfaces, we can write the response in the frequency domain as

$$\begin{aligned} W(\mathbf{X}_0, \omega) &= \iint \text{plane waves} \\ &= \int_{-\infty}^{\infty} \int_{-\infty}^{\infty} S(\omega) \cdot F(\mathbf{p}_A) \cdot \Pi(\mathbf{p}_A) \\ &\quad \cdot \exp\left[i\omega \left(\mathbf{p}_A \cdot \mathbf{X}_A + \mathbf{p}_B \cdot \mathbf{X}_B + \sum_{\text{ray}} \xi_j z_j \right) \right] \cdot C(\mathbf{p}_B) \cdot dp_x dp_y. \quad (20) \end{aligned}$$

Here, $S(\omega)$ is the source spectrum; $F(\mathbf{p}_A)$ is the radiation pattern; $\prod(\mathbf{p}_A)$ is the product of transmission coefficients appropriate to the generalized ray path; and $C(\mathbf{p}_B)$ is a receiver-dependent factor that is appropriate for the particular response under analysis (e.g., the vertical displacement, or a particular strain component). The double integral is thought of as a decomposition of the source into its plane wave components, recombining these plane waves after their passage through the medium. It is necessary to find the “along-interface” slownesses to evaluate factors within $\prod(\mathbf{p}_A)$, and also to find \mathbf{p}_B as a function of \mathbf{p}_A . However, as shown above in equations (4) through (9), this can be done systematically in a way that does not require raytracing. The distances $\mathbf{X}_0, \mathbf{X}_A, \mathbf{X}_B$ in equation (20) are independent of \mathbf{p}_A .

We can show that the double integral in equation (20) has a stationary integrand for the special value of slowness \mathbf{p}_A that does shoot a ray from A (the source) to B (the receiver). The demonstration requires a notation that distinguishes between the fixed value of \mathbf{X}_B , and a functional relationship such as $\mathbf{X}_B(\mathbf{p}_A)$ or $\mathbf{X}_B(\mathbf{p}_B)$, giving the dependence of range on slowness. Let us loosely use $\mathbf{X}_B(\mathbf{p})$ to refer to either of the latter functions.

Thus, defining

$$J = \mathbf{p}_A \cdot \mathbf{X}_A + \mathbf{p}_B \cdot \mathbf{X}_B + \sum_{\text{ray}} \xi_j z_j \quad (\mathbf{X}_A \text{ and } \mathbf{X}_B \text{ fixed}), \tag{21}$$

and substituting for $\sum_{\text{ray}} \xi_j z_j$ from equation (3), we have

$$J = T - \mathbf{p}_B \cdot [\mathbf{X}_B(\mathbf{p}) - \mathbf{X}_B(\text{fixed})]. \tag{22}$$

Let us now make a small perturbation from \mathbf{p}_A to $\mathbf{p}_A + \Delta\mathbf{p}_A$, and consider the effect on J in equation (22). Note that \mathbf{X}_A is still fixed, because this merely specifies the position (with respect to the source) at which “layer thicknesses” are defined. But the dependent variables $\mathbf{p}_B, T, \mathbf{X}_B$ and J become $\mathbf{p}_B + \Delta\mathbf{p}_B, T + \Delta T, \mathbf{X}_B + \Delta\mathbf{X}_B$, and $J + \Delta J$. From any of the Figures 1 through 5, it is clear that (to first order) $\Delta T = \mathbf{p}_B \cdot \Delta\mathbf{X}_B$. It follows that

$$\begin{aligned} J + \Delta J &= T + \Delta T - (\mathbf{p}_B + \Delta\mathbf{p}_B) \cdot [\mathbf{X}_B(\mathbf{p}) + \Delta\mathbf{X}_B - \mathbf{X}_B(\text{fixed})] \\ &= J - \Delta\mathbf{p}_B \cdot [\mathbf{X}_B(\mathbf{p}) - \mathbf{X}_B(\text{fixed})]. \end{aligned} \tag{23}$$

Hence,

$$\Delta J = 0 \quad \text{if } \mathbf{X}_B(\mathbf{p}) = \mathbf{X}_B(\text{fixed}), \tag{24}$$

and so the integrand of (20) has stationary phase, for the slowness value that shoots a ray to the actual position of the receiver.

Parts of this analysis are similar to ideas contained in Frazer and Phinney (1980) and Burdick and Salvado (1986), notably our equation (22). However, a key part is different in that the concept of a sum over vertical slownesses is retained even for a 3-D varying medium. The phase within equation (20) can easily and exactly be computed via (21), which in turn has an interpretation in terms of rays and stationary points, via (22). Much can therefore be retained, of the decades of experience in understanding waves in plane-parallel layering.

A SIMPLE EXAMPLE

In order to verify at the simplest level one of the most elementary uses of the method given above and to suggest further improvements, we can compare the method with exact ray theory for the reflections from a single-dipping layer. We compare reflection travel times, horizontal slownesses, and geometrical spreading for the situation shown in Figure 10 (500 m source-receiver distances) and Figure 11 (2500 m). These calculations were done for the same discretized "look-up" table for $\sum_{\text{ray}} \xi_j z_j$, using the range ± 0.2 sec/km with 40 points for each of the two cartesian components of \mathbf{p}_A . We see from Figure 10 that travel-time errors begin to show in the fifth significant digit; horizontal slowness errors in the third significant digit; and geometrical spreading errors in the second significant digit. Errors are seen to be somewhat larger for Figure 11, although still insignificant for most practical purposes.

Our numerical method is based on finding the six unknown constants in equation (17). For Figures 10 and 11 we have taken a primitive approach, merely generalizing to 2-D the 1-D exercise described by equations (12) and (13). We may presume that a more sophisticated fit to the sampled J function (J is linearly related to the sampled τ function) would result in improved accuracy, perhaps with opportunities for working with a coarsely sampled table of $\tau = \sum_{\text{ray}} \xi_j z_j$ values.

DIPPING SOURCE/RECEIVER STRUCTURE IN A SPHERICAL EARTH

Teleseismic pulse shapes for P waves and SH waves, in the distance range $30^\circ < \Delta < 90^\circ$ and for the band from about 0.01 to 2 Hz, are often satisfactorily modeled by geometrical ray theory in a spherically symmetric Earth. Using this simple framework, together with allowance for a source region that may have finite spatial and temporal extent, produces fits to both pulse shape and absolute amplitude that are remarkably good for many events. But such success raises questions as to why good fits are not always achievable for signals in this distance range and bandwidth.

We presume the answer is, in part, that lateral structure at source and receiver has an influence, as shown for example by Wiens (1987, 1989), who interpreted teleseismic P waves that had been affected by shallow-dipping sea-floor. He obtained synthetics by using a raytracing method described by Langston (1977).

We here outline a practical approach to implementing geometrical ray theory for teleseismic pulse shapes when shallow structure has layers with several dipping planar interfaces. Thus, we are interested in the effect of structures near source and receiver as shown in Figure 12, for body waves that propagate mostly in spherically symmetric parts of the Earth.

If the problem shown in Figure 12 were addressed via an Earth-flattening transformation of the spherical structure, with horizontal distance \mathbf{X} between vertical reference lines (which would now be parallel), then it is appropriate to take

$$J = \mathbf{p}_A \cdot \mathbf{X}_A + \mathbf{p} \cdot \mathbf{X} + \mathbf{p}_B \cdot \mathbf{X}_B + \sum_{\text{boxes}} \xi_j z_j + \int \xi dz, \quad (25)$$

where \mathbf{p} is the constant horizontal slowness vector throughout the 1-D part of the structure. The integral in equation (25) is taken over that range of depths

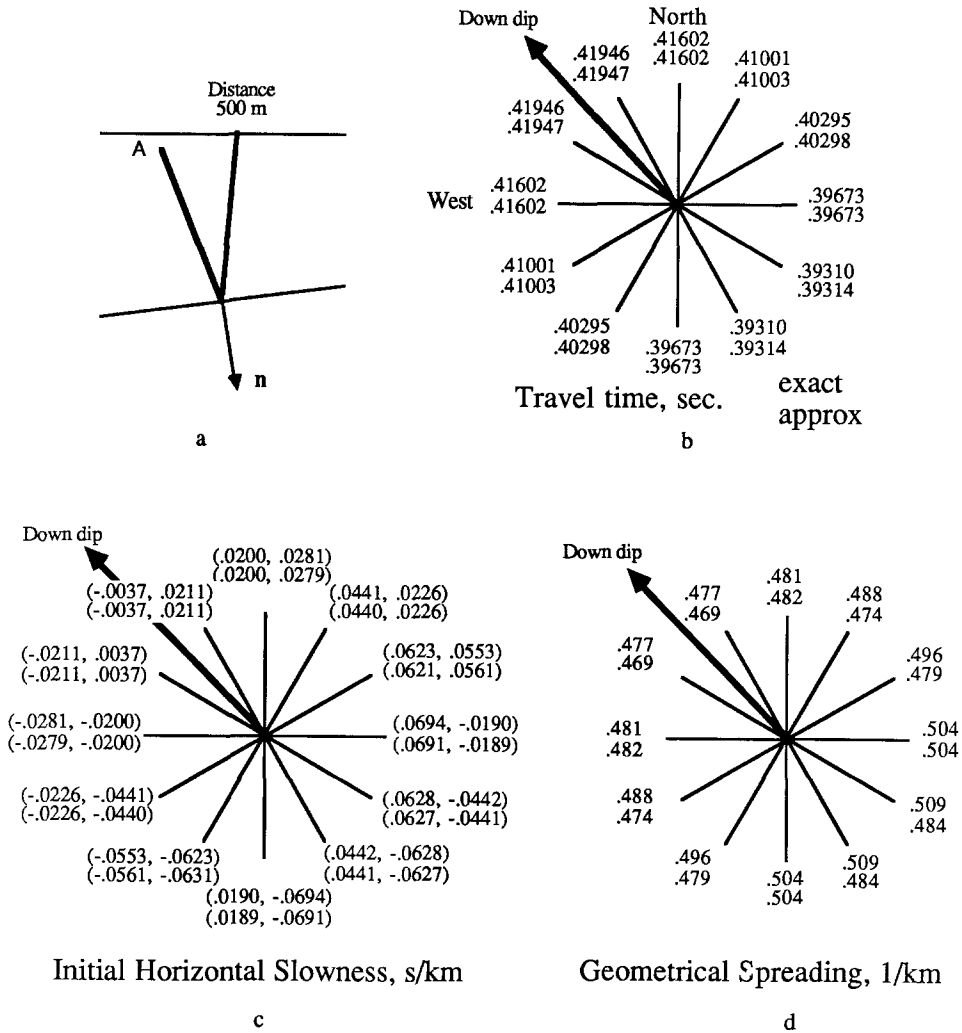
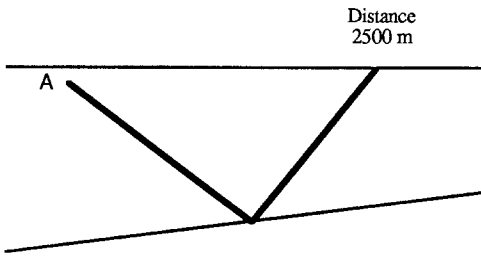


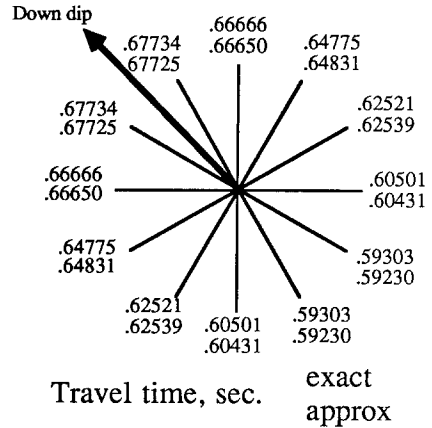
FIG. 10. Computation for the reflection from a layer dipping to the NW. (a) shows the source (depth 10 m); the layer (*P*-wave speed 5 km/sec); the reflector (*n* defined as in Fig. 2 has components 0.1 in both the south and east directions, and the reflector is 1000 m deep at the point vertically below *A*); and a typical receiver. (b), (c), and (d) are map views of the receivers, all at the same range but spaced around the source azimuthally in 30° increments. Upper numbers are exact (to number of significant digits shown), lower numbers are derived from the method of this article. (b) shows travel times, (c) initial slownesses, and (d) geometrical spreading. For a horizontal reflector at the same depth below the source, travel time would be 0.41037 sec; geometrical spreading would be 0.487 km⁻¹.

spanned by the ray within the laterally homogeneous regions, in which $\xi = \sqrt{1/v(z)^2 - p_x^2 - p_y^2}$. Equation (25) is a further generalization of Diebold's (1987) result and is in a form that may be adapted to the global spherical geometry of Figure 12. For example, $\int \xi dz$ in (25) would be replaced by $\int \xi dr$ (integrating over the range of radii spanned by the ray in the spherically symmetric part of the Earth model), with $\xi = \sqrt{1/v(r)^2 - p_{\text{sph}}^2/r^2}$ and p_{sph} = spherical ray parameter.

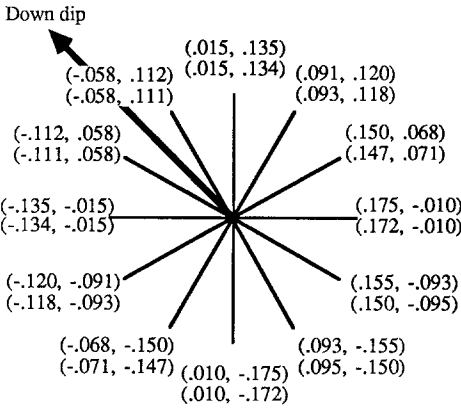
In working sequentially along the ray from source to receiver, we may take p_A as the independent variable specifying the take-off direction on the focal



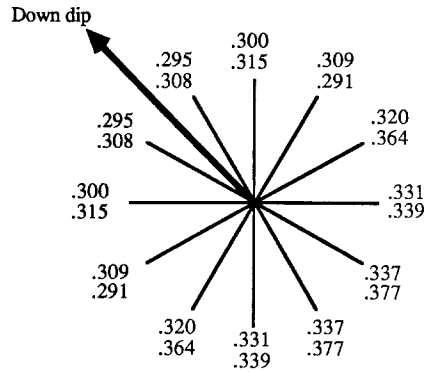
a



b



c



d

FIG. 11. Computation for the reflection from a dipping layer. As in Figure 10, except that the receivers are 2500 m horizontally from the source. For a horizontal reflector at the same depth below the source, travel time would be 0.63906 sec; geometrical spreading would be 0.313 km⁻¹.

sphere and follow the sequence of equations (4) through (9) for ray segments in the source-region box until the ray is passed downward (across interface i , say) into the spherically symmetric region. The associated ray parameter needed in equation (25) is $p_{sph} = |\mathbf{p}_i| r_a$, in units of sec/radian. Passing back into cartesian at the receiver region, the box containing B , horizontal slownesses begins with magnitude p_{sph} / r_b and is in the direction that is both horizontal and in the same vertical plane as \mathbf{p}_i . The sequence of slownesses is then continued in local cartesian until reaching the receiver at B .

For purposes of evaluating the integral representation of the wave field, equation (20), there are three reasons to integrate over \mathbf{p} in (25), rather than using \mathbf{p}_A as the independent variable. First, this allows a further simplifying interpretation of \mathbf{p} in terms of its amplitude (scalar ray parameter) and az-

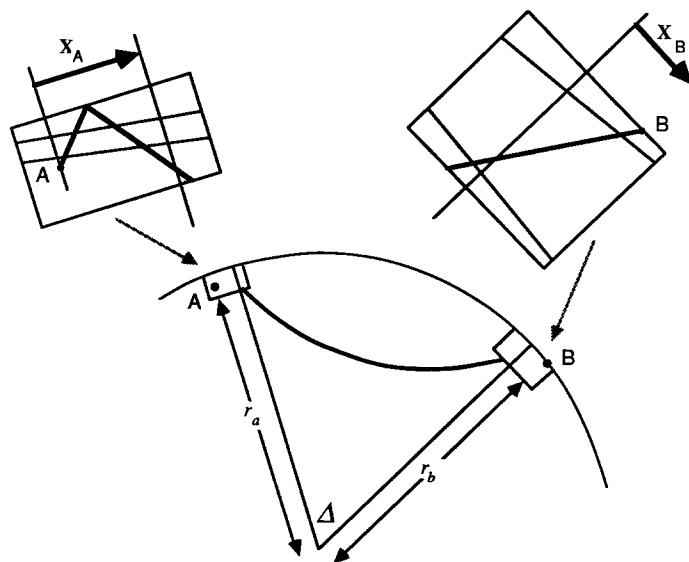


FIG. 12. Dipping structures with planar layering are shown at source and receiver, in boxes embedded within a spherically symmetric Earth. Each box has a vertical reference line, used both to define "layer thicknesses," and X_A or X_B . The Figure is a 2-D schematic of a 3-D problem. Although it is inconsistent to treat the lower surface of each box as part of a cartesian system and part of a spherical surface, the effect is insignificant in practice.

imuth, facilitating the connection between Earth-flattened and spherical structures. The integral over azimuth of \mathbf{p} , in the spherical case, introduces a factor $1/\sqrt{\sin \Delta}$ rather than $1/\sqrt{\Delta}$. Second, the search for stationary values of J in equation (25) is made easier if J is regarded as a function of \mathbf{p} rather than \mathbf{p}_A , because the desired location (in slowness space) will be close to the point that gives a stationary value for the corresponding 1D problem (i.e., with all dips set to zero). Third, our preliminary studies indicate that it may often be possible to obtain values of the integral in equation (20) quite easily as a function of the location of stationary points in the \mathbf{p} plane (specified by amplitude and azimuth). The integral is approximated as a product of factors, some tabulated (by carrying out a stationary phase integral) for a particular spherically symmetric Earth model, and others evaluated numerically for the particular near-source or near-receiver structure of interest. For example, once the \mathbf{p} value at which $J(\mathbf{p})$ is stationary is known, one can easily obtain the corresponding values of \mathbf{p}_A and the Jacobian relating changes in \mathbf{p} to changes in \mathbf{p}_A . From these, one can quantify the effects of the radiation pattern and of near-source structure on overall geometrical spreading.

An example of the outcome is described in Figure 13, showing the P wave that would be recorded at a distance of 50° for eight different azimuths from a strike slip earthquake with hypocenter 6 km below the ocean floor. Synthetics for this problem were given by Wiens (1987) using a raytracing method. We show seismograms that are built up from direct P , plus the pP and sP reflections from the water/crust interface, plus two sets of multiples of water reverberation, namely: pwP , pwP , etc., up to pwP ; and swP , swP , etc., up to swP (up to 14 water legs in each set), for a total of 31 generalized rays. The case of a flat-lying ocean floor is compared with a floor that dips 1° or 2° , and as noted by Wiens there is great

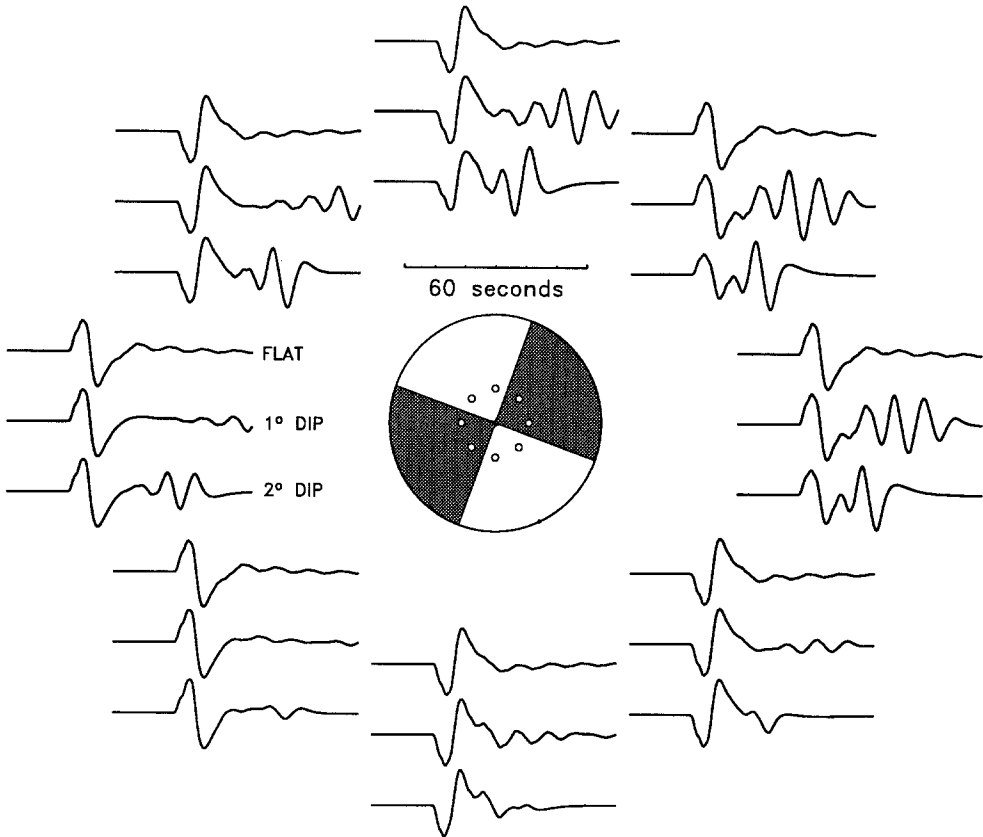


FIG. 13. *P*-wave synthetics for azimuthally distributed WWSSN long-period seismograms, from a strike-slip earthquake beneath the ocean floor that is either flat or slightly dipping (to the east). The spherically symmetric part of the Earth is modeled by PREM, with $t^* = 1$; the source time function is a trapezoid of 4-sec total duration (1 sec up, 2 sec flat, 1 sec down).

sensitivity of waveforms to small dip angles. Not all these rays exist at all azimuths. Computation is via an evaluation of equations (20) and (25), and our synthetics agree well with those obtained by Wiens (1987) using a raytracing method for this problem.

DISCUSSION

We have shown how a generalized ray theory may be developed for media built up from homogeneous layers separated by planar interfaces. We have also suggested a primitive method for obtaining such basic properties as travel times and geometrical spreading, although the integral for a generalized ray equation (20), can be evaluated in many other ways. As with generalized ray theory for horizontal plane layering, there is always the question of choosing which generalized rays are significant.

The problem of fitting the correct rays between a predetermined source and a set of receivers has a long history in seismology, and we have claimed at several stages during the above exposition that our method does not require raytracing through the medium of interest. We can contrast this with the so-called “shooting” or “bending” methods described (for example) in Aki and Richards (1980,

Section 13.1). There is, of course, the need to track changes in horizontal slowness at each interface along a generalized ray, for each discrete initial slowness value in a “look-up” table. But this differs from raytracing in that the look-up table need be computed only once and then would be usable for different sources and receivers.

The essential reason why the 3-D method described here can be so efficient, avoiding raytracing in the usual sense, is that there is still an underlying lateral invariance even if each planar interface has different dip and strike. The invariance arises in the way that the sequence of slowness vectors along a generalized ray depends only on the sequence of wave speeds in each layer and on the orientation of interfaces met by the ray. Specifically, these slowness vectors do not depend on source/receiver locations or layer thicknesses, so they can be stored and used for a variety of different problems. Physically, we can see this invariance is a direct consequence of the planar nature of each interface: If the orientation of a ray segment in one of the layers is specified, the orientation of all other ray segments (for a particular generalized ray) is determined and is independent of where the original ray segment actually is, within its layer. However, note that, in complicated media where some layers pinch out or interfaces change direction abruptly, there may be the need to ensure that the generalized ray of interest does indeed interact with interfaces as expected. To make this point, consider the situation shown in Figure 14. The relevant form for the generalized ray response, equation (20), in this case would appear to require extra information concerning the range of horizontal ray parameters, since the reflected ray is lost as horizontal slowness is increased. To understand these situations, some type of raytracing check may be helpful (after a stationary ray has been found).

Apart from the forward calculation of pulse shapes in a given structure, two other major applications for our 3-D formalism may be noted. The first, described briefly by Diebold (1989), is inversion to obtain thickness of each layer and the strike and dip of its lower surface; the second is event location.

Thus, from an array of geophones it is possible to measure travel times as a function of horizontal slowness, and hence to evaluate $\tau = \tau(\mathbf{p})$ where \mathbf{p} is a 2-vector. Interpreting τ as $\sum \xi_j z_j$, Diebold (1989) discussed a τ - \mathbf{p} inversion to obtain the characteristics of each 3-D layer. Concerning event location, the primary need in practice is to be able to compute rapidly the travel times from trial hypocenters to a given set of stations, and thus to form residuals that are systematically reduced by iterating. As shown in different ways by Buland and

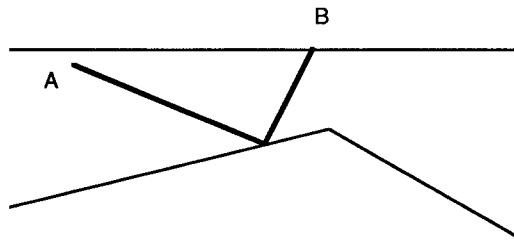


FIG. 14. A ray departing from *A* is reflected from a locally plane interface and received at *B*. But this reflection would not be expected to be present at much greater distances, since the reflector would be missed by rays departing nearly horizontally from *A*.

Chapman (1983) and Tralli and Johnson (1986), the key is to have a table of τ values at discrete values of horizontal slowness.

The basic reason why inversion methods and event location methods make use of τ is that this quantity summarizes all the information about Earth structure needed for purposes of interpreting travel times and other ray properties. Thus, study of the τ quantity represents an intermediate stage, whether going from structure to synthetics (τ is computed from $\sum \xi_j z_j$), or going from seismic signals to structure (τ is estimated from the data). This has long been known for 1-D problems, has in recent years been shown for 2-D, but is also true for 3-D problems with planar interfaces.

ACKNOWLEDGMENTS

We thank John Diebold for discussions which sparked this investigation, and David Simpson and Art Lerner-Lam for reviews of a draft ms. This research was supported by NSF Grant EAR 87-08564. Lamont-Doherty Contribution 4706.

REFERENCES

- Adachi, R. (1954). On a proof of fundamental formula concerning refraction method of geophysical prospecting and some remarks, *Kumamoto J. Sci., Ser. A* **2**, 18-23.
- Aki, K. and P. G. Richards (1980). *Quantitative Seismology: Theory and Methods*, 2 vol., W. H. Freeman, San Francisco.
- Borcherdt, R. D., G. Glassmoyer, and L. Wennerberg (1986). Influence of welded boundaries in an elastic media on energy flow, and characteristics of *P*, *S*-I, and *S*-II waves: observational evidence for inhomogeneous body waves in low-loss solids, *J. Geophys. Res.* **91**, 11503-11518.
- Buland, R. and C. H. Chapman (1983). The computation of seismic travel times, *Bull. Seism. Soc. Am.* **73**, 1271-1302.
- Burdick, L. J. and C. A. Salvado (1986). Modeling body wave amplitude fluctuations using the three-dimensional slowness method, *J. Geophys. Res.* **91**, 12482-12496.
- Chapman, C. H. (1976). A first motion alternative to geometrical ray theory, *Geophys. Res. Lett.* **3**, 153-156.
- Chapman, C. H. and J. A. Orcutt (1985). The computation of body wave synthetic seismograms in laterally homogeneous media, *Rev. Geophys.* **23**, 105-163.
- Diebold, J. D. (1987). Three-dimensional travel time equation for dipping layers, *Geophysics* **52**, 1492-1500.
- Diebold, J. B. (1989). Tau-*p* analysis in one, two and three dimensions, in *Tau-*p*: A Plane Wave Approach to the Analysis of Seismic Data*, Paul L. Stoffa (Editor), Kluwer, Hingham, Massachusetts, 71-117.
- Diebold, J. B. and P. L. Stoffa (1981). The traveltime equation, tau-*p* mapping and inversion of common midpoint data, *Geophysics* **46**, 238-254.
- Frazer, L. N. and R. A. Phinney (1980). Computation of body wave synthetic seismograms in a laterally varying medium, *Geophys. J. R. Astr. Soc.* **63**, 691-717.
- HelMBERGER, D. L. (1968). The crust-mantle transition in the Bering Sea, *Bull. Seism. Soc. Am.* **58**, 179-214.
- Hong, T.-L. and D. L. HelMBERGER (1977). Generalized ray theory for a dipping structure, *Bull. Seism. Soc. Am.* **67**, 995-1008.
- Johnson, S. J. (1976). Interpretation of split-spread refraction data in terms of plane dipping layers, *Geophysics* **41**, 418-424.
- Langston, C. A. (1977). The effect of planar dipping structure on source and receiver responses for constant ray parameter, *Bull. Seism. Soc. Am.* **67**, 1029-1050.
- Richards, P. G. (1973). Calculation of body waves, for caustics and tunnelling on core phases, *Geophys. J. R. Astr. Soc.* **35**, 243-264.
- Richards, P. G. (1984). On wavefronts and interfaces in anelastic media, *Bull. Seism. Soc. Am.* **74**, 2157-2165.
- Richards, P. G. (1985). Seismic wave propagation effects: development of theory and numerical modelling, in *The VELA Program: A Twenty-Five Year Review of Basic Research*, A. U. Kerr (editor), Executive Graphic Services, Arlington, Virginia, 183-251.

- Spencer, T. W. (1960). The method of generalized reflection and transmission coefficients, *Geophysics* **25**, 625-641.
- Tralli, D. M. and L. R. Johnson (1986). Estimation of travel times for source location in a laterally heterogeneous Earth, *Phys. Earth Plan. Interiors* **44**, 242-256.
- Wiens, D. A. (1987). Effects of near source bathymetry on teleseismic *P* waveforms, *Geoph. Res. Lett.* **14**, 761-764.
- Wiens, D. A. (1989). Bathymetric effects on bodywaveforms from shallow subduction zone earthquakes and application to seismic processes in the Kurile trench, *J. Geophys. Res.* **94**, 2955-2972.
- Wiggins, R. A. (1976). Body wave amplitude calculations. II, *Geoph. J. Roy. Astr. Soc.* **46**, 1-10.

LAMONT-DOHERTY GEOLOGICAL OBSERVATORY
COLUMBIA UNIVERSITY
PALISADES, NEW YORK 10964
(P.G.R., D.C.W., G.E.)

DEPARTMENT OF GEOLOGICAL SCIENCES
COLUMBIA UNIVERSITY
PALISADES, NEW YORK 10964
(P.G.R., D.C.W)

Manuscript received 19 April 1990